Low-frequency elastic shear constant and low-temperature configuration of $K_{1-x}Li_xTaO_3$

1991 J. Phys.: Condens. Matter 3 8377

(http://iopscience.iop.org/0953-8984/3/43/005)

J. Phys.: Condens. Matter 3 (1991) 8377–8385. Printed in the UK

Low-frequency elastic shear constant and low-temperature configuration of $K_{1-x}Li_xTaO_3$

Ulrich T Höchli†, Joachim Hessinger‡ and Klaus Knorr‡

† IBM Research Division, Zurich Research Laboratory, CH-8803 Rüschlikon, Switzerland

‡ Institute of Physics, University of Mainz, D-W 6500 Mainz, Federal Republic of Germany

Received 28 May 1991, in final form 23 July 1991

Abstract. Elastic shear constant data are presented for $K_{1-x}Li_xTaO_3$ at very low frequencies near the transition temperature to a glass phase. A comparison made with dielectric-susceptibility data reveals the character of the relaxation modes. The low-temperature state is described in terms of short dipolar but long quadrupolar correlation.

1. Introduction

$K_{1-x}Li_xTaO_3$ is considered to be a prototype dipole glass [1, 2], at least for Li concentrations below some 4%. The Li ions replace K at an off-centre position in an oxygen cage of cubic symmetry. It thus carries a dipole moment $p_i = ex_i$ and a quadrupole moment $q_{ij} = ex_ix_j$ where $i, j = 1, 2, 3$. In a polarizable lattice, these moments need not be the same as the bare moments. While the enhancement factor for dipole moments in $KTaO_3$ is well established, there appears to be no relationship between the bare electric quadrupole moment and the (dressed) elastic quadrupole moment in a crystal. At small concentrations where these moments do not interact, a change of Li position, say from x to y, entails a change of a dipole moment and quadrupole moment at the same time. Dipole and quadrupole moments occupy random sites where the interaction is also random and, accordingly, the ground state is disordered.

It was pointed out long ago that the direct interaction between the Li moments may be modified [3] by the lattice polarizability which for $KTaO_3$ is unusually high: $\epsilon = 4000$ at low temperatures. This modification was shown to lead to an enhancement of the quadrupole interaction at sufficiently high concentration. The condition for this to happen is an enhancement of the polar correlation length of the host lattice to the nearest-neighbour impurity distance. According to this view $K_{1-x}Li_xTaO_3$ (KTL(x)) would be an ordered ferroelastic for $x > x_c$. Extended to dipolar interactions [2, 4], however, its validity appears to be limited to lattice sites devoid of inversion symmetry [5, 6]. If dipolar interaction had an ordered component, then the ground state of KTL(x) would be ferroelectric.

Despite numerous experimental investigations on KTL(x) the complexity arising at high x is still a source of dispute [1, 2]. On the basis of dielectric relaxation and nuclear magnetic resonance data [7] it has been suggested that a transition [8] occurs from

0953-8984/91/438377+09$03.50

a dipole glass state to an 'ordered' state at $x \simeq 0.04$. Qualitative changes between low-x and high-x behaviour have also been reported in x-ray scattering [9] and in birefringence studies [10, 11]. On the other hand, experiments on Raman scattering [12], Brillouin scattering [13] and second-harmonic light generation [10] appear not to distinguish any differences in the qualitative behaviour in these concentration ranges.

The essential feature of a condensed state of moments is the slowing down in the mode of motion as the temperature T is reduced. Its symmetry and strength determines the configuration of the frozen moments. Li ions are displaced with respect to the centrosymmetric site. The displacement, and hence the dipole moment, points in the direction of a fourfold crystallographic axis. Reorientation is possible by $\pi/2$ and π motion. Assume that the $\pi/2$ motion of independent polar moments slows down until the moments have a static orientation. Then, if their orientation is $+z$ at some position, there is an equal probability for neighbouring moments to be oriented along the $+z, -z, +x, -x, +y$ and $-y$ axes. The fact that birefringence is observed, together with the results from numerous other experiments mentioned earlier, forces us to discard this simple hypothesis. Apparently KTL is less random than a Heisenberg spin glass [14] but it is also less ordered than a ferroelectric crystal.

To determine the mechanisms that lead to the peculiar ground state of KTL we wish to present data on millihertz acoustic dispersion. These data will be correlated with published data from experiments performed at higher frequencies as well as with data on dielectric dispersion. The interpretation of these results will give us some insight into the delicate balance between ordering and disordering (also called frustrated [14]) interaction.

2. Experimental details

We investigated two crystals: the $K_{0.966}Li_{0.034}TaO_3$ crystal was grown by spontaneous nucleation while the $K_{0.93}Li_{0.07}TaO_3$ crystal was grown by the Czochralski technique. No systematic dependence of dielectric properties on the growth method is reported and the Czochralski method appears to be suited for the growth of larger specimens, especially at a high Li concentration.

Both crystals have the shape of a column with a quadratic cross section of 1 mm $\times$1 mm and a height of 6 mm and 2 mm, respectively. The long axis is along [110]. The crystal was glued onto the cold plate of a closed-cycle refrigerator with a permanent magnet and a mirror on its free end. A torque parallel to [110] is applied to the crystal via an external magnetic field H. The resulting shear angle α, detected by the deflection of a laser beam from the mirror, is proportional to an inverse elastic shear constant c_s [15]. For the chosen geometry c_s is a function of c_{44} and $(c_{11} - c_{12})/2$ [16].

Based on the available information [17] on the elastic constants of c_{44} and $(c_{11} - c_{12})/2$ of the tantalates we feel justified in assuming that all dispersion effects will be due to the E_g component $(c_{11} - c_{12})/2$.

Varying the magnetic field sinusoidally with frequencies between 0.05 and 0.6 Hz, the real part of c, Re(c), can be determined by the inverse amplitude of the laser beam deflection, whereas Im(c) is determined by the phase angle between the response and the external torque.

In figure 1, we plot the phase angle θ against temperature for $K_{0.966}Li_{0.034}TaO_3$ at three different frequencies. The frequency span from 0.05 to 0.6 Hz is not sufficient to allow standard fits to expressions of the form $\psi(\omega)$ as obtained from relaxation models

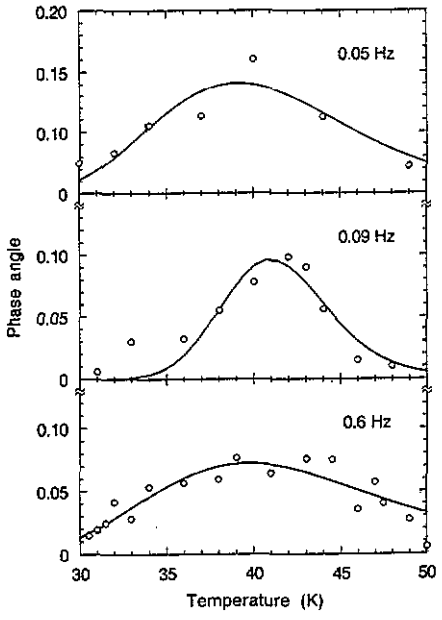

Figure 1. Phase shift between deflection of torsion pendulum and applied AC torque against T at various frequencies, interpreted as the ratio between the imaginary and real part of the elastic shear constant. Full curve, fit of data to $\tan\theta = \int d\ln(\tau) g(\tau) \Delta c\, \mathrm{Im}(1 - j\omega\tau)/[(c - \Delta c)\,\mathrm{Re}(1 - \omega\tau)]$, where $g(\tau) = \pi^{-1/2}\Delta^{-1} \exp -(\ln\tau - \ln\tau_0)^2/\Delta^2$, $\ln\tau_0 = \ln\tau_\infty + E_b/kT$. $E_b/k = 1150 \pm 50$ K, $\Delta = 5 \pm 1.5$, $\Delta c = 0.38 \pm 0.05$. The sample is $K_{0.966}Li_{0.034}TaO_3$.

[18]. Guided by the results on dielectric relaxation [19] we *assume* that relaxation rates are log-normally distributed (width Δ) around a mean value which is given by the Arrhenius expression $\tau_0 = \tau_\infty \exp(E_b/kT)$. The value for τ_∞ is taken from a fit of high-frequency data [19] to an Arrhenius function; we set $\ln\tau_\infty^{-1} = 31.9$. We may thus attempt to fit the data for the phase angle to

$$\tan\theta = \int d\ln(\tau) g(\tau) \Delta c\, \mathrm{Im}(1 - j\omega\tau)/[(c - \Delta c)\,\mathrm{Re}(1 - j\omega\tau)]$$

where reference [20]

$$g(\tau) = \pi^{-1/2}\Delta^{-1} \exp[-(\ln\tau - \ln\tau_0)^2/\Delta^2] \qquad \ln\tau_0 = \ln\tau_\infty + E_b/kT.$$

Here, c is the shear elastic constant in the absence of dispersion and Δc the elastic dispersion step. We determine the dispersion step and its width Δ as well as the barrier height E_b for each frequency measured. They should be independent of frequency; indeed if we allow an uncertainty of background of $\tan\psi \simeq 0.005$ and an uncertainty of the T measurement of 0.5 K on different runs, we obtain, with internal consistency, $E_b = 1150 \pm 50$ K, $\Delta c = 0.38 \pm 0.05$, and $\Delta = 5.5 \pm 1.5$, valid in a narrow temperature range centred around 40 K.

Analogous plots of the inverse amplitude of the pendulum are given in figure 2. The findings are similar: higher frequencies shift the response to higher temperatures, apparently without changing the shape of the response term. No fit was attempted since the unknown background elastic constant introduces two more fit parameters.

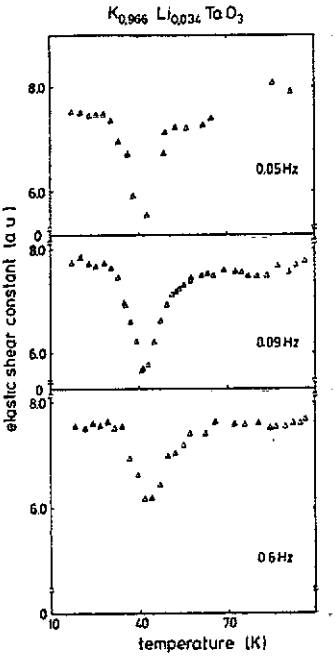

Figure 2. Reciprocal amplitude of torsion pendulum against T, interpreted as being the real part of the elastic shear constant at various frequencies; the sample is $K_{0.966}Li_{0.034}TaO_3$.

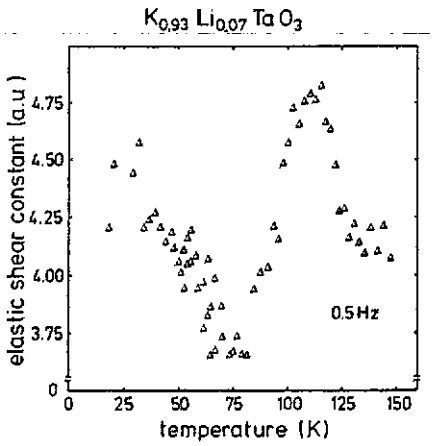

Figure 3. Real part of the elastic shear constant against T, measured at a frequency of 0.5 Hz; sample is $K_{0.93}Li_{0.07}TaO_3$.

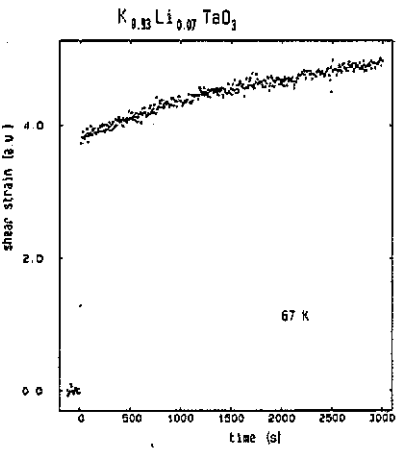

Figure 4. Deflection of the torsion pendulum against time after application of a steady torque at $t = 0$ at a temperature of 67 K.

Similar data are reported for $K_{0.93}Li_{0.07}TaO_3$ in figure 3 near 75 K. In view of the limited sample dimension, the deflection amplitudes were reduced which resulted in a large relative scatter. Hence, no frequency dependence was resolved. Instead we measured the torsion as a function of time after applying a torque at $t = 0$ and

$T = 67$ K. The result is shown in figure 4. Clearly, relaxation is much slower than at 75 K. From these data we were able to estimate the size of the elastic dispersion step and the dominant relaxation rate, given by the frequency ω of the maximum phase angle. The relaxation rates are summarized in figure 5 in an Arrhenius diagram $\ln \tau^{-1}$ against T^{-1}. In the same diagram we have plotted the relaxation rates determined from ultrasonic transmission data [17, 18] on similar samples. The dielectric properties are also displayed and it is striking that the whole data set can be described in terms of two relaxation branches, a rapid one with a slope of $\partial \ln \tau / \partial (T^{-1}) = 1150$ K, and a slow one with a slope of 2300 K. We have also summarized the dispersion steps from the pendulum experiment at 40 K, from dielectric [19] and acoustic [18] measurements at higher T. The result is shown in figure 6(a) for the lower concentration and in figure 6(b) for the higher concentration. The results shown in figure 5 immediately appeal to the intuition and confirm the prediction that the Arrhenius slopes represent barriers against $\pi/2$ and π reorientation of moments. The results in figure 6 require a more detailed consideration on which we now embark.

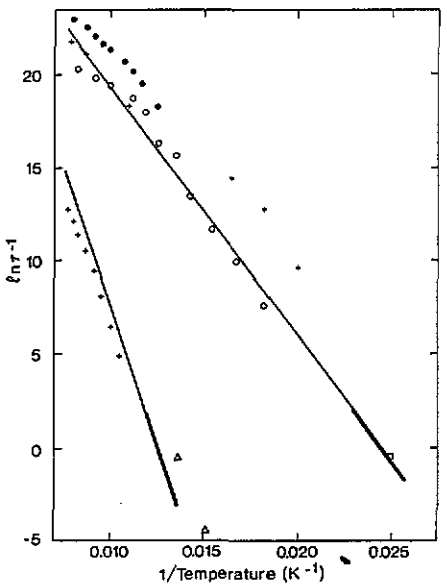

Figure 5. Leading relaxation rates τ^{-1} against temperature in an Arrhenius plot: $\ln \tau^{-1}$ against T^{-1}: ○, dielectric, 3.4% [18]; □, torsion pendulum, 3.4% (this work); +, dielectric, 7% [18]; ●, acoustic, 5% [17, 19]; △, torsion pendulum, 7% (this work). The straight lines are plots of the Arrhenius law $\tau^{-1} \simeq \exp(-E_b/kT)$: bold, from the torsion pendulum; faint, extrapolation to high temperature, indicating compatibility with ultrasonic data. $E_b/k = 1150$ K for the rapid relaxation branch, $\tau_0' = 2\pi \times 10^{13}$ s^{-1}. For the slow relaxation branch $E_b/k = 2100$ K in agreement with dielectric data from [7, 21].

3. Interpretation

We start by identifying the nature of the relaxation branches in KTL(3.4). We note that the acoustic and dielectric relaxation rates of the rapid branch are the same and the amplitudes are mutually proportional between 70 and 120 K. From this we

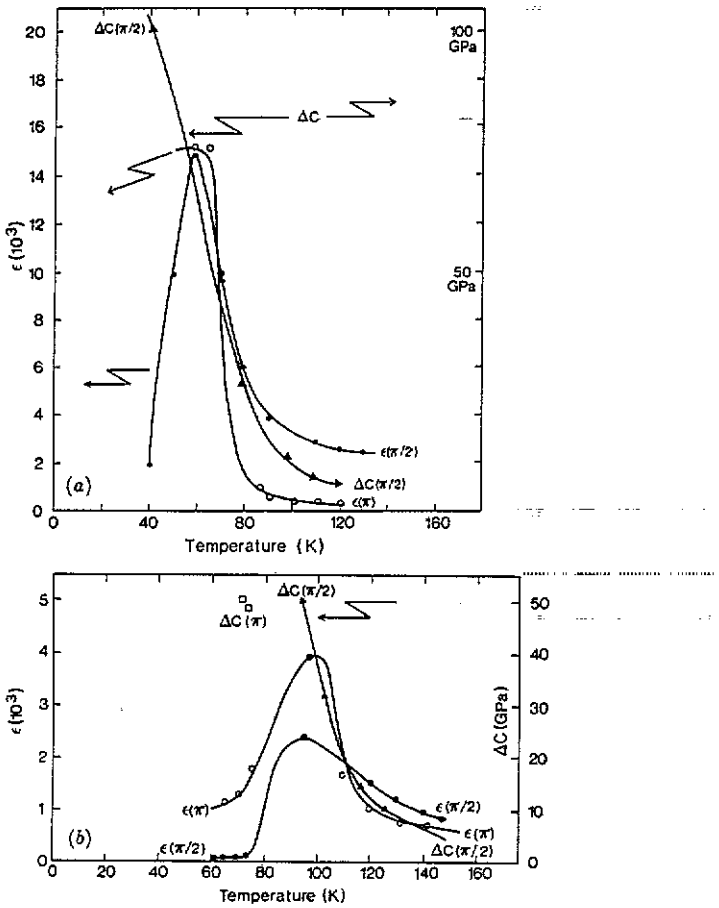

Figure 6. Ultrasonic and dispersion steps for the various relaxation modes (*a*) $K_{0.966}Li_{0.034}TaO_3$, and (*b*) $K_{0.93}Li_{0.07}TaO_3$: Δ, $(\pi/2)$ motion, sound experiment [19]: ●, $(\pi/2)$ motion, dielectric experiment [18]; ○, (π) motion dielectric [18]; ■, $(\pi/2)$ motion, torsion pendulum; and □, (π) motion, torsion pendulum.

conclude that the quadrupole and dipole moments of Li have identical behaviour and the motion is by $\pi/2$ since motion by π would leave the quadrupole moment invariant. We identify the upper branch as being due to $\pi/2$ motion, not only between 70 and 120 K, but also at its extrapolation to 40 K. The torsion data are thus to be interpreted in terms of $\pi/2$ reorientation. Inspection of figure 6 informs us, however, that the acoustic dispersion continues to rise whereas dielectric dispersion becomes progressively quenched as T drops. The way to reconcile these findings is to assume that below about 70 K, $\pi/2$ motion is collective, i.e. in clusters, and that a cluster contains dipoles on parallel and antiparallel alignment. Its total dipole moment is thus reduced by compensation whereas the total quadrupole moment is still the sum of all individual quadrupole moments. The rise of quadrupolar dispersion indicates that, as the cluster size increases, the quadrupolar correlation length should exceed the dipolar correlation length approximately in proportion to the relative dispersion amplitude.

There is a dielectric relaxation branch not associated with acoustic relaxation. It is

readily associated with the π motion of moments. Where it has appreciable strength, at approximately 60 K, it is 10^6 times slower than the $\pi/2$ motion. Apparently, an occasional cluster finds it more advantageous to flip directly by π than to take the detour over two nominally lower $\pi/2$ barriers.

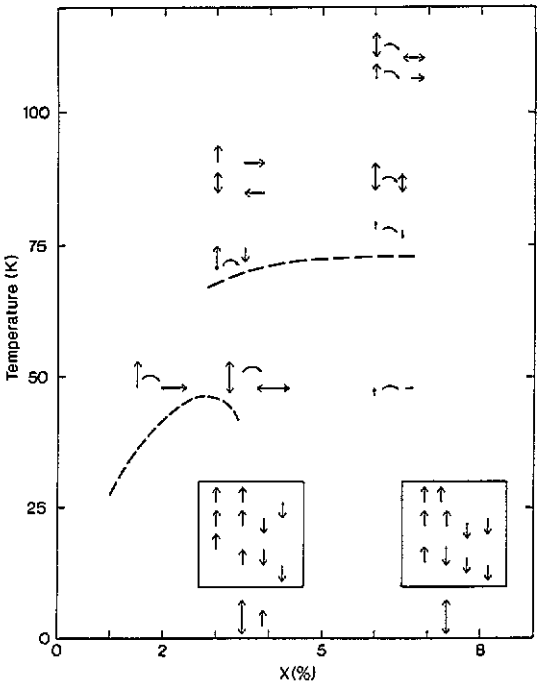

Figure 7. Freezing temperature of dominating relaxation modes and low-temperature configuration: arrow, dipole moment; double-arrow, quadrupolar moment. Size indicates dispersion strength. The framed array of dipoles is a cluster; below the frame the total moment of the cluster is shown. Note the compensation of the dipolar contribution at large x.

The data taken on the heavily-doped sample KTL(7) have considerable scatter. In order to establish the nature of the minimum of the elastic susceptibility at 75 K, $f = 0.09$ Hz we have performed a real-time relaxation experiment which established $\tau \simeq 10^{+3}$ s at 67 K. The data establish the dynamic nature of the elastic response in KTL(7) as well. We note that the relaxation rate group near the lower, slow, branch for dielectric relaxation (figure 5) is not associated with acoustic relaxation at high T; hence, relaxation should be by π motion, i.e. inversion of the dipoles. The observation of an acoustic response on this branch at low T is at first surprising. To give rise to an acoustic response, the total quadrupole moment must change its magnitude upon inversion. A single Li impurity cannot produce such an effect by symmetry. Therefore this observation is to be attributed to the loss of local inversion symmetry of the lattice caused by the large Li concentration. Below approximately 70 K there is almost no evidence for $\pi/2$ motion; it apparently takes too much energy for a cluster to assume an orientation perpendicular to its neighbours.

We now return to these results in terms of a phase diagram T against x (figure 7). For low x, say below 1%, $\pi/2$ motion is dominant, and each moment freezes into a

random position without establishing correlation. The low-temperature configuration is dominated by single-ion freezing and is sometimes called a 'glassy crystal' [1]. For concentrations larger than 1%, up to about 3.4%, $\pi/2$ motion is predominant. It established quadrupolar correlation. Slow π-motion becomes progressively important and dipolar correlation increases with x.

At 7% Li, π motion is dominant at all temperatures below 100 K. The motion of these clusters is indicated by arrows in figure 7 and the ensuing static configuration is also sketched.

These results appear to be consistent with experiments on second-harmonic light generation [10]: the static quadrupolar correlation exceeds the dipolar correlation by several orders of magnitude and both grow with concentration. It is also consistent with x-ray scattering data [9] which show dipolar correlation in excess of the coherence length of the x-ray (a few 1000 Å) at 5% Li but not at 1.7%. Brillouin [13] and Raman [12] scattering data imply quadrupolar correlation exceeding the wavelength of light as well, and birefringence studies have revealed quadrupolar correlation sometimes extending to macroscopic lengths. The model prediction that best accounts for the enhancement of quadrupolar correlation is that by Vikhnin and Borkovskaya [3]: The polar mode at the origin of the instability of the $KTaO_3$ host forces the impurity moments to stay parallel to the lattice displacements, i.e. $\pm z$. It thus aligns the quadrupole moment in a range given by the correlation length of the polarizable $KTaO_3$ host.

4. Conclusion

The two elastic dispersion steps observed in the relaxation experiments using a torsion pendulum have the following origin: in KTL(3.4), the elastic response indicates that clusters of Li moments relax over $\pi/2$ barriers. The moments are of quadrupolar and dipolar nature but, within the cluster, there is substantial reduction of the total dipole moment due to their parallel–antiparallel alignment. The reduction becomes progressively important as T drops and x increases. In KTL(7) the $\pi/2$ feature is not observed at 40 K, but at 73 K a relaxation step emerges and is attributed to inversion flips of Li moments by π. The fact that strong acoustic dispersion is observed implies that the plus–minus positions of the cluster are inequivalent. Electrical moments are suppressed in magnitude due to local compensation. At all concentrations except at the limit $x \rightarrow 0$, the ground state has a quadrupolar correlation length exceeding the dipolar correlation length by several orders of magnitude. The dynamical mechanism leading to this configuration, however, changes rather abruptly at $x \simeq 0.04$: at concentrations below 0.04, freezing $\pi/2$ motions establish both quadrupolar alignment and dipolar twinning near T_f whereas at concentrations above 0.04, dipolar twinning is established by $\pi/2$ motion. With increasing Li concentration, this motion becomes weak, but now slow, far above T_f. Near T_f, quadrupolar alignment is provided by a mode which implies π motion and whose symmetry reflects distortion of the host lattice by the numerous Li defects. Both the strength of the π motion and the relaxation time appear to rise monotonically with decreasing T and do not diverge at some critical temperature. Accordingly the low-temperature configuration of KTL(7) should be attributed to a quadrupolar glass rather than to a ferroelastic or ferroelectric.

References

[1] Höchli U T, Knorr K and Loidl A 1990 *Adv. Phys.* **39** 605
[2] Vugmeister B E and Glinchuk M D 1990 *Rev. Mod. Phys.* **62** 993
[3] Vikhnin V S and Borkovskaya Y B 1978 *Sov. Phys.–Solid State* **20** 2082
[4] Vugmeister B E and Glinchuk M D 1979 *Sov. Phys.–Solid State* **21** 735
[5] Höchli U T and Maglione M 1989 *J. Phys.: Condens. Matter* **1** 2241–56
[6] Stachiotti M G, Migoni R L and Höchli U T 1991 *J. Phys.: Condens. Matter* **3** 3689
[7] van der Klink J J, Rytz D, Borsa F and Höchli U T 1983 *Phys. Rev.* B **27** 89
[8] Höchli U T and Baeriswyl D 1984 *J. Phys. C: Solid State Phys.* **17** 311
[9] Andrews S R 1985 *J. Phys. C: Solid State Phys.* **18** 1357
[10] Azzini G A, Banfi G P, Giulotto E, Höchli U T 1991 *Phys. Rev.* B **43** 7473
[11] Kleemann W, Kütz S, Schäfer F J and Rytz D 1988 *Phys. Rev.* B **37** 5856
[12] Prater R L, Chase L L and Boatner L A 1981 *Phys. Rev.* B **23** 221; 1981 *Phys. Rev.* B **23** 5904
[13] Chase L L, Lee E, Prater R L and Boatner L A 1982 *Phys. Rev.* B **26** 2759
[14] Binder K and Young A P 1986 *Rev. Mod. Phys.* **58** 801
[15] Hessinger J and Knorr K 1989 *Phys. Rev. Lett.* **63** 2749
[16] Voigt W 1928 *Lehrbuch der Kristallphysik* (Berlin: Teubner) (reprint of 1st edn, 1910)
[17] Höchli U T, Weibel H E and Rehwald W 1982 *J. Phys. C: Solid State Phys.* **15** 6129
[18] Doussineau P, Levelut A, Ziolkiewicz S and Höchli U T 1991 *J. Phys.: Condens. Matter* **3** 8369–75
[19] Christen H M, Höchli U T, Châtelain A and Ziolkiewicz S 1991 *J. Phys.: Condens. Matter* **3** 8387–401
[20] Wagner K W 1913 *Ann. Phys., Lpzg.* **40** 817
[21] Höchli U T, Grymaszewski E and Hutton S L 1990 *J. Phys.: Condens. Matter* **2** 4259